

# DFT Calculations of Unpromoted and Promoted MoS<sub>2</sub>-Based Hydrodesulfurization Catalysts

Line S. Byskov,<sup>\*</sup> Jens K. Nørskov,<sup>\*</sup> Bjerne S. Clausen,<sup>†</sup> and Henrik Topsøe<sup>†</sup>

<sup>\*</sup> Center for Atomic-Scale Materials Physics, Department of Physics, Technical University of Denmark, DK-2800 Lyngby, Denmark; and <sup>†</sup>Haldor Topsøe Research Laboratories, Nymøllevvej 55, DK-2800 Lyngby, Denmark

Received February 15, 1999; revised June 3, 1999; accepted June 7, 1999

Self-consistent density functional theory (DFT) is used to study the structure and active sites in unpromoted and promoted MoS<sub>2</sub>-based hydrodesulfurization (HDS) catalysts. A model consisting of single-layer MoS<sub>2</sub> chains with and without promoter atoms located at the edges is used to represent the structures in the catalysts, and full relaxation is allowed to find the lowest energy configurations. The results show that the most favored edge structures deviate significantly from those considered in the literature and those expected from simple terminations of the bulk MoS<sub>2</sub> structures. The calculations also show that the promoter atoms prefer to be located at the so-called sulfur-terminated (1010) MoS<sub>2</sub> edges. Although such structures have not been considered previously, it is found that they are in agreement with available structural information from Extended X-Ray Absorption Fine Structure (EXAFS) experiments. Since the creation of sulfur vacancies is believed to be the first step for many hydrotreating reactions, the energy required to remove sulfur from the different structures has also been calculated. Comparison with catalytic activity results for MoS<sub>2</sub>, Co–Mo–S, Ni–Mo–S, and Fe–Mo–S structures shows that the highest HDS activity is obtained for the structures with the lowest metal sulfur binding energy, in general agreement with the bond energy model (BEM). A more detailed analysis of the sulfur bonding in promoted MoS<sub>2</sub> structures based on a simple LCAO-type model explains the origin of the different promotional behaviors. Finally, the adsorption of hydrogen on the different structures is discussed. We find hydrogen adsorption at edge sulfur atoms to be strong, and suggest that the S-edge is partly covered by SH groups during catalysis. © 1999

Academic Press

## 1. INTRODUCTION

Hydrodesulfurization (HDS) has for many years been one of the most important areas in catalysis (1). In recent years, this field has attracted increased interest due to the introduction of new environmental legislation requiring further reduction in the sulfur contents of oil products. In many areas of the world, the maximum allowed amount of sulfur is announced to be 50 ppm. These new requirements will have large consequences for the refineries. Significant efforts will have to be devoted to improving the processes

and introducing new and more active catalysts which are optimized to treat the molecular species dominating under deep HDS conditions (1–8).

In order to aid the development of catalysts for HDS, there has been a strong emphasis in the past on establishing fundamental relationships between the structure of the catalyst and the HDS activity (1). For unpromoted Mo catalysts, the activity has been related to sites at the MoS<sub>2</sub> edges, whereas for the Co and Ni promoted catalysts the presence of promoter edge atoms in the Co–Mo–S and Ni–Mo–S type structures has been observed to play a key role. For many catalyst systems, direct relationships have been established between the catalytic activity and the number of such edge promoter atoms. In spite of the significant progress in understanding HDS catalysts, many fundamental questions regarding the active sites in MoS<sub>2</sub> and the promotional effect are still being debated (1, 9, 10).

It is generally believed that fully coordinated metal atoms in sulfided catalysts will be unable to adsorb sulfur-containing molecules, and the number of sulfur vacancies may thus be a key measure of the catalytic activity. Clearly, other features will be important, but it has been shown (11–13) in the framework of the bond energy model (BEM) that trends in HDS activity for both transition metal sulfides and Co–Mo–S type structures can be explained considering the variations in the metal–sulfur bond strength (or the tendency to form vacancies). A key problem has been how to determine the metal–sulfur bond strength. In the original BEM, which nicely describes the large activity variations for many sulfide systems, *ab initio* band structure calculations were used as a basis for estimating the metal sulfur binding energy. It was also shown that good activity correlations could be obtained simply by using the heat of formation of the bulk sulfides (normalized per mole sulfur) as an estimate of the metal–sulfur binding energy. The advantage of using the BEM is that it provides an insight into the physical properties which determine the metal–sulfur binding energy. Thus, the model could also be used to estimate the effect of adding promoters on the HDS activity. Nevertheless, it should be pointed out that the BEM and

many other previous models (see, e.g., (1) and (13) for a discussion) uses bulk properties for the sulfides for estimating the energetics of vacancy formation, and such models are therefore not expected to give an accurate description of the processes occurring at the catalyst surface. Thus, these models are probably best suited for looking at overall trends in activity variations.

In view of the above limitations, there is a need to obtain a more detailed description of the structure and bonding properties of the active catalyst edge structures. In the literature it has generally been assumed that the  $\text{MoS}_2$  edge structure is similar to those derived from simple terminations of the bulk  $\text{MoS}_2$  structure (see, e.g., (1) for a discussion). The active sites are then typically derived by removal of different combinations of the singly or doubly bound sulfur atoms. In the present paper, the nature and stability of different  $\text{MoS}_2$  and Co–Mo–S type edges are investigated by means of self-consistent density functional theory (DFT) calculations. In recent years, it has been demonstrated that theory and in particular DFT calculations are able to provide a wealth of new insight into many catalyst systems, including systems relevant to HDS (13–23). We have previously described preliminary results from DFT calculations on HDS catalysts (13, 15, 16), and in the present paper we will discuss these as well as new results in more detail.

## 2. CALCULATION METHOD

In the fully self-consistent density functional theory (DFT) calculations (24), the exchange-correlation energy is described nonlocally by the generalized gradient approximation (GGA) (25). The ionic cores are modelled by pseudopotentials. We have used two types, soft (26) and ultrasoft (27) pseudopotentials. The former allow us to expand the wave functions in plane waves with a cutoff energy of 40 Ry for sulfided Mo structures, and 50 Ry for configurations including Co, Ni, and Fe that all have more tightly bound  $d$ -states, while for the latter type of pseudopotentials a cutoff of 25 Ry is enough to get convergence in binding energies. The binding energies differ by less than 0.1 eV for the two types of pseudopotentials, but in any case we have marked the results in all tables and figures with (S) for soft and (US) for ultrasoft pseudopotentials. The results presented are also not strongly dependent on the choice of nonlocal exchange-correlational potential (24).

We perform a complete structural relaxation of all configurations. The occupation numbers are Fermi distributed with an electronic temperature of  $kT = 0.025$  eV. The total energies are extrapolated to  $T = 0$  K.

In the literature, the nature of the edge termination of the sulfided Mo-based catalyst has been discussed extensively. Two principally different types of edges are possible, (1) an Mo terminated ( $10\bar{1}0$ ) edge and (2) an S terminated ( $\bar{1}010$ )

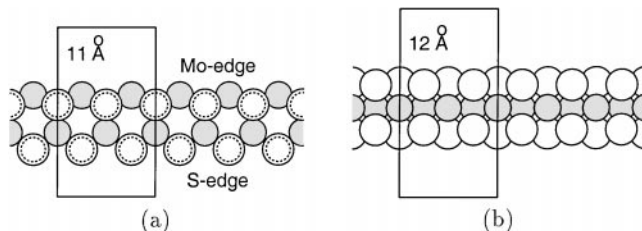


FIG. 1. The stoichiometric  $\text{MoS}_2$  chain model. White and light grey circles denote S and Mo atoms, respectively. Dashed circles indicate S atoms in the bottom layer. The super cell is indicated by a rectangular box. (a) Top view. (b) Side view from the S-edge.

edge. The simplest model including the two edges is a chain-like structure, as depicted in Fig. 1. The starting point is a stoichiometric  $\text{MoS}_2$  model, but in the presence of  $\text{H}_2\text{S}$  in the gas phase this may not be the most stable structure. To study this, we therefore add S atoms to the edges. As seen from Fig. 1, the S-edge is covered by the largest possible amount of S atoms, but at the Mo-edge another two S atoms per Mo edge atom can be added. The bonding of the S atoms to the two edges can hence be calculated by removal of one S atom at a time.

By the setup in Fig. 1, periodic boundary conditions can be applied, both along the chains and in the other two perpendicular directions. In the latter two, the chains are repeated with a periodicity of 12 Å perpendicular to the  $\text{MoS}_2$  planes and 11 Å perpendicular to the edges. This distance is chosen to be large enough that the interactions between chains can be neglected. To correct for the difference in the dipole moments of the S- and Mo-edges, a dipole layer is added between the chains.

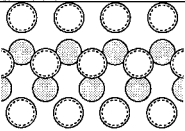
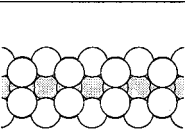
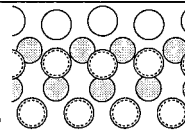
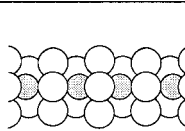
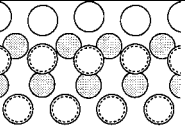
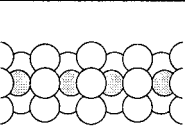
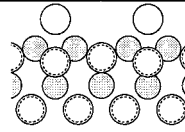
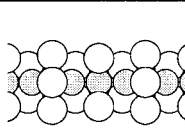
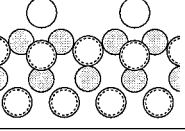
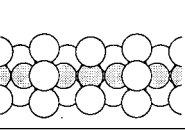
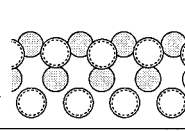
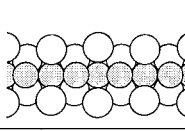
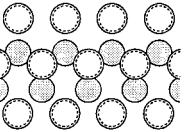
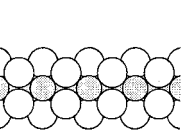
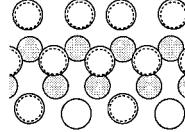
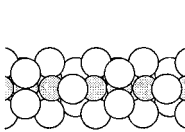
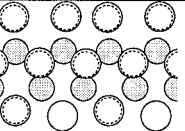
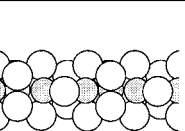
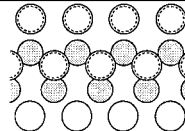
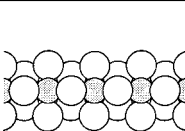
In the following, we consider two different chain structures. We first study the simplest model which has a width of only two Mo (or Co) metal atoms (called “2 Mo”), but to test the dependence of the results on the width of the chains we also consider a three metal atom wide chain (called “3 Mo”).

The DFT calculations describe bulk systems excellently. The calculated equilibrium lattice constants are 3.11 Å for Mo metal, 2.52 Å for Co metal, and  $d_{\text{Mo-Mo}} = 3.12$  Å for  $\text{MoS}_2$  (15). In comparison, the experimental values are 3.15 (28), 2.51 (29), and 3.16 Å (30). Raybaud *et al.* have also shown that trends in bulk structures and heats of formation for all the transition metal sulfides are well described in DFT (17). In the present work, the calculated lattice constant of the  $\text{MoS}_2$  (bulk) system is used as starting input before relaxation of the structures.

For  $\text{MoS}_2$  systems promoted with Co and Fe, we have investigated the effect of spin polarization. For Co–Mo–S structures, total energies are found to change only by 0.01–0.02 eV when spin polarizing the structure. Co–Mo–S and Fe–Mo–S configurations with one vacancy (see Section 6 and Fig. 3) are calculated to have a low magnetic moment

TABLE 1

MoS<sub>2</sub> Structures before and after Removal of Sulfur Atoms (The Corresponding Sulfur Binding Energy (per Sulfur Atom) Is Given. White and Light Grey Circles Denote S and Mo Atoms, Respectively. Dashed Circles Indicate S Atoms in the Bottom Layer. (US).)

Mo-edge				
Initial		Final		$\Delta E_S$
Top View	Side View	Top View	Side View	(kJ/mol)
				14
				57
				246
S-edge				
Initial		Final		$\Delta E_S$
Top View	Side View	Top View	Side View	(kJ/mol)
				13
				140

of 0.02 and 0.38  $\mu_B$  per Co or Fe atom, respectively.<sup>1</sup> Spin polarization has an insignificant effect on the sulfur binding energy,  $\Delta E_S$  (defined in Section 3, Eq. [1]), which in both cases is changed only by about 0.01 eV ( $\approx 1$  kJ/mol). In the following, we therefore only consider unpolarized structures.

### 3. STRUCTURE AND SULFUR BONDING OF THE MoS<sub>2</sub> CATALYST

The equilibrium structure of the MoS<sub>2</sub> chain is found by setting up a number of different structures and allow-

<sup>1</sup> Magnetic susceptibility measurements on unsupported Co-promoted MoS<sub>2</sub> have revealed a slightly higher magnetic moment of 0.37  $\mu_B$  at 5 K (31). These experiments were not carried out under true *in situ* conditions, and hence it cannot be ruled out that a small part of the Co atoms has been oxidized to a high-spin cobalt species resulting in a higher average magnetic moment.

ing these to relax towards the minimum energy configuration.

After adding the maximum possible number of S atoms to the stoichiometric structure in Fig. 1, the resulting, equilibrium structure after relaxation is structure *a* in Table 1. It is interesting that the sulfur atoms are seen not to occupy the normal lattice positions at the edges. It is seen that the S atoms have a tendency to dimerize at both edges. At the S-edge, there is a local minimum in which the S atoms are close to the perfect lattice position; however, this configuration is meta-stable relative to the dimerized structure. At the Mo-edge, the nondimerized structure is extremely unstable, since the S atoms coordinate to only a single Mo atom. Although typically previous studies (see (1)) assume S in normal lattice positions, experimental studies using Raman spectroscopy (32) and X-ray photoelectron spectroscopy (XPS) (33, 34) have in fact also given indications for the presence of disulfide species in the catalysts.

### 3.1. Sulfur Bonding

Sulfur bonding to the edges is now investigated in more detail. The sulfur binding energy,  $\Delta E_S$ , is defined as

$$\Delta E_S = E(\text{chain with vacancy}) + E(\text{H}_2\text{S}) - E(\text{chain}) - E(\text{H}_2). \quad [1]$$

By removing the S atoms one by one and calculating  $\Delta E_S$  for each removal, we can identify the structure which is expected to dominate under usual gas-phase  $\text{H}_2/\text{H}_2\text{S}$  ratios. In addition, such calculations provide information on the energy required to remove S atoms from the most stable structure, and this may, as discussed in the introduction, be related to the probability of creating active sites on the catalyst.

Removal of a single S atom from the Mo-edge is energetically expensive (13). If, however, one vacancy can be created per Mo edge atom (going from *a* to *b* in Table 1), the net energy cost per removed S atom is only 14 kJ/mol. The reason that a half-stripped edge is so relatively stable is that it restructures completely. All S atoms move half a lattice constant along the chain to become twofold coordinated. Note that the coupling between stability and reconstruction means that this structure is only stable if the whole edge is stripped.

Creating further vacancies at the Mo-edge is moderately expensive up to the point when one S is removed per two Mo atoms (Table 1, *c*). Removing more S atoms is energetically very expensive.

At the S-edge, creation of the first vacancy to make structure *e* in Table 1 requires nearly no energy. Further removal of S atoms from the S-edge is, however, energetically unfeasible. It can be seen from structure *e* for the S-edge that large restructuring also accompanies S removal from this edge. When one of the S atoms is removed, the one below it flips up into the plane of the Mo atoms. None of the reconstructions at the S-edge are collective like in structure *b*

at the Mo-edge. This means that, e.g., double vacancies can be made without having to reconstruct the whole edge.

The picture that emerges is one in which the Mo-edges of the working catalyst are filled by one or two sulfur atoms per Mo edge atom. Either way the Mo atoms are fully coordinated by six sulfur atoms. Vacancies created at the S-edges apparently provide the most easily accessible coordinatively unsaturated Mo atoms.

We have also tried to see if coordinatively unsaturated Mo atoms could be produced by removing S atoms from the basal plane of  $\text{MoS}_2$ . We found that  $\Delta E_S = 217$  kJ/mol in this case, supporting the notion that the basal planes are inactive in HDS (35).

Structures *a* and *b* in Table 1 are quite different from previous models of active  $\text{MoS}_2$  catalysts (see, e.g., (1)). The structure is nonstoichiometric and has S restructuring at both edges. The structure we find appears, however, to be compatible with available experimental observations. EXAFS typically shows a sulfur coordination number of six (1, 30). This does not support a stoichiometric model with bare Mo-edges, but it is in good agreement with our model with both S dimers and monomers at the Mo edge. The present model also gives good agreement with experiments regarding bond lengths, which we will return to below.

We have investigated the effect of the number of S atoms at one edge on the S bonding on the other edge. We find this effect to be weak even for the very narrow structure considered here.

To investigate if the width of the chain has an effect on the properties of the edges, we have also studied structures which are three Mo atoms wide. We first consider a "3 Mo" structure without vacancies as depicted in Table 2. Just as for the "2 Mo" structure, the S atoms at both the Mo-edge and the S-edge dimerize. At the S-edge the nondimerized structure is a local minimum, but it is 47 kJ/(mol unit cells) higher in energy than the dimerized structure.

Next, we investigate the case of "3 Mo" structures having one vacancy at the S-edge as depicted in Table 2. The

TABLE 2

**MoS<sub>2</sub> Structures before and after Removal of Sulfur Atoms (The Sulphur Binding Energy (per Sulfur Atom) Is Given. White and Light Grey Circles Denote S and Mo, Respectively. Dashed Circles Indicate S Atoms in the Bottom Layer. (US.)**

S-edge, "3 Mo"				
Initial		Final		$\Delta E_S$ (kJ/mol)
Top View	Side View	Top View	Side View	
				-11

TABLE 3

Calculated Average Bond Lengths for Nearest Neighbor Atoms in MoS<sub>2</sub> and Co-Mo-S Structures (“3 Mo” and “2 Mo” Refer to Structures that Are Two and Three Mo Atoms Wide, Respectively; See Fig. 2. For Co-Mo-S with H, No Vac. Refers to Structure *h* in Table 8, and with Vac. Is Structure *g* in Table 8.) Experimental Values: <sup>1</sup>(37), <sup>2</sup>(38, 39), <sup>3</sup>(39)

Bond	Bond Lengths (Å)							
	Experimental Values		MoS <sub>2</sub> No Vacancies		Co-Mo-S With Vacancies		Co-Mo-S with H	
	MoS <sub>2</sub>	Co-Mo-S	“3 Mo”	“2 Mo”	“3 Mo”	“2 Mo”	No Vac.	With Vac.
Mo-S	2.41 <sup>1</sup>	2.41 <sup>1</sup>	2.44	2.44	2.41	2.39	2.41	2.47
Co-S	–	2.18–2.28 <sup>2</sup>	–	–	2.24	2.23	2.24	2.25
Mo-Mo	3.16 <sup>1</sup>	3.16 <sup>1</sup>	3.10	2.97	3.11	2.86	2.98	2.95
Co-Mo	–	2.80–2.87 <sup>3</sup>	–	–	2.96	2.79	3.17	2.77
S-H	–	–	–	–	–	–	1.36	1.36

sulfur binding energy,  $\Delta E_S$ , is found to be  $-11$  kJ/mol. This is about 20 kJ/mol smaller than the value calculated for the “2 Mo” structure, showing that the width has some effect on the calculated bond strengths. The effect of the width is, however, small compared to the differences in S bonding energies for different structures in Table 1, and it is comparable to the intrinsic accuracy of the exchange-correlation description used (which is of the order 20 kJ/mol).

### 3.2. Interatomic Distances

We now turn to the investigation of the interatomic distances in the MoS<sub>2</sub> configurations. Table 3 compares calculated bond lengths for the “2 Mo” and “3 Mo” structures with and without vacancies with bond lengths extracted from EXAFS experiments. These studies give average distances for the small MoS<sub>2</sub> structures that are close to the bulk values. Top views of the structures are shown in Fig. 2. In general, the calculated and experimental interatomic distances agree very well. The calculated bond lengths for the “3 Mo” MoS<sub>2</sub> slab agree quite well with those found for the outermost layers of MoS<sub>2</sub> structures studied by Raybaud *et al.* (39). The only significant deviation from the experimental values is the Mo-Mo bond length in the “2 Mo” structure, which is too small. This could indicate that Mo is typically present in larger structures in the catalysts. The “2 Mo” structure is too narrow to have any “bulk-like” Mo and therefore contracts. The “3 Mo” is, however, wide enough not to have this feature, and here the agreement with the experiment is excellent. We note that even though the “2 Mo” structure has a too-small Mo-Mo bond length, the S bond strength and general structure is still well described. We are therefore concentrating on the “2 Mo” structures for the rest of the present work.

We will return to the question of the effect of Co promoters and adsorbed hydrogen below.

### 4. LOCATION OF Co IN THE Co-Mo-S STRUCTURE

The Co promoted MoS<sub>2</sub> catalysts are the most commonly applied and experimentally studied HDS catalysts (1). It has been established experimentally that the Co atoms are

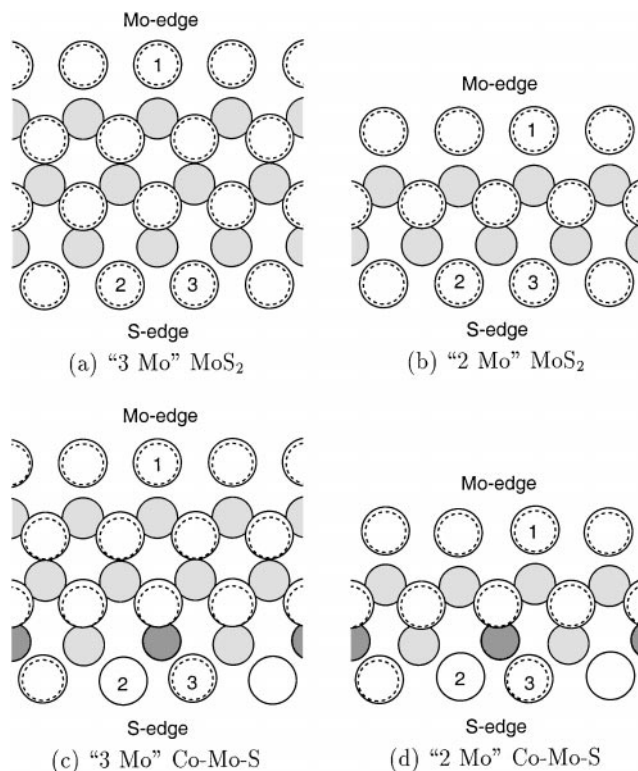


FIG. 2. Top views of structures, which are (a), (c) three Mo atoms and (b), (d) two Mo atoms wide. White, light grey, and dark grey circles denote S, Mo, and Co atoms, respectively. Dashed circles indicate S atoms in the bottom layer. For MoS<sub>2</sub> structures: Atoms 1–3 are present in S dimers. For Co-Mo-S structures, atom 3 is in an S dimer, while atom 2 is a single S atom (near the vacancy).

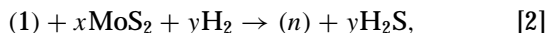
located at the edges of the MoS<sub>2</sub> particles in so-called Co–Mo–S structures, but the exact structural environment of the Co atoms and their role are still being debated extensively (1, 10). This has motivated studies of (i) the location of the Co atom in the Co–Mo–S structure (Section 4.1 and 5), (ii) the stability of Co–Mo–S (Section 4.2), (iii) the role of other promotor atoms (Section 6), and (iv) the effect of atomic hydrogen (Section 7).

#### 4.1. Possible Co–Mo–S Structures

We have studied seven different possible locations of Co at the MoS<sub>2</sub> edges, and the Co–Mo–S structures are shown in Table 6. The number  $n$  refers to the configuration number in Table 6, and structure 1 is used as a reference, i.e., all other structures are compared with this one.

The most stable configuration is the structure with the lowest energy. However, it is not possible to compare the energies of 1–7 in Table 6 directly because of the difference in the total number of S and Mo atoms (per super cell) in the different structures.

We therefore use the reaction energy of the following reaction to compare structures with different numbers of atoms,



and the energy difference is hereby

$$\Delta E_n = E(n) + yE(\text{H}_2\text{S}) - E(1) - xE(\text{MoS}_2) - yE(\text{H}_2). \quad [3]$$

The terms  $E(n)$  and  $E(1)$  correspond to the total energy of configurations  $n$  and 1, respectively.  $E(\text{MoS}_2)$  is the calculated total energy of an MoS<sub>2</sub> bulk system, and  $E(\text{H}_2)$  and  $E(\text{H}_2\text{S})$  are calculated energies of the free molecules. Reaction [2] describes the equilibrium between the different Co containing structures and bulk MoS<sub>2</sub> in an H<sub>2</sub>/H<sub>2</sub>S gas flow.

A positive value of  $\Delta E_n$  implies that the left side of reaction [2] is the most stable. It is in fact seen that  $\Delta E_n$  is positive for all the structures 2–7. From this we can conclude that configuration 1 in Table 6 with Mo substituted by Co at the S-edge is the most stable structure of the seven studied Co–Mo–S types. This Co atom is seen to have a sixfold coordination in the sulfided Co–Mo structure. It is noteworthy that configuration 6, which is the structural model of Co–Mo–S favored previously in the literature (37, 38, 40–43), is not the most stable structure. In this model, the promotor atom Co is believed to be located at the edges in fivefold coordinated sites at the (10 $\bar{1}$ 0) edge planes of MoS<sub>2</sub>. These Co sites have tetragonal pyramidal-like (t-pyr) geometry, and the singly bonded S atom is located in the plane of Mo. It should also be noted that the presence of corner sites in cluster-shaped particles may give rise to sites for the Co atoms that may have slightly different surroundings compared to the ones considered above.

We have also considered the two most stable structures 1 and 4 from Table 6 with vacancies. Table 5 shows that even with a vacancy at either the Mo-edge or at the S-edge the configuration with Co at the S-edge is most stable. In fact, the energy difference in Table 5 is close to the difference between the similar structures 1 and 4 in Table 6.

#### 4.2. Stability of Co–Mo–S Relative to CoS

A key question for several years has been whether Co atoms in the Co–Mo–S structure are stable relative to Co<sub>9</sub>S<sub>8</sub> (see, e.g. (1, 10, 44)). To investigate this we have calculated the relative stability of Co in the two phases. For simplicity we study CoS instead of the Co<sub>9</sub>S<sub>8</sub> phase. We can do this because CoS is only marginally less stable than Co<sub>9</sub>S<sub>8</sub> (17). We calculate

$$\Delta E = E(\text{Mo}_4\text{S}_{12}) + E(\text{CoS}) - E(\text{MoS}_2) - E(\text{CoMo}_3\text{S}_{11}), \quad [4]$$

which is the reaction energy of the reaction



The quantities that enter reaction [5] are the layered disulfide, MoS<sub>2</sub>, which here describes the basal plane of the catalyst, CoMo<sub>3</sub>S<sub>11</sub>, which is the vacancy-containing Co–Mo–S type structure depicted in Fig. 3, Mo<sub>4</sub>S<sub>12</sub>, which has no vacancies and exposes edges as shown in Table 1,  $a$  and CoS, a monosulfide which is a hexagonal nickel arsenide type structure (45).

It can be seen that if  $\Delta E > 0$ , the side with the Co–Mo–S phase is the more stable. From our calculations, we find  $\Delta E$  to be 125 kJ/mol; hence the Co–Mo–S phase is the more stable one.

### 5. STRUCTURE AND SULFUR BONDING OF THE Co–Mo–S CATALYST

Having established the location of the Co atom in the sulfided Co–Mo–S structure (see configuration 1 in Table 6, Section 4) we can now study the effect of Co on the S vacancy formation energy to obtain a model of the Co–Mo–S catalyst. If Co lowers  $\Delta E_S$ , the number of active sites will increase, explaining (at least partly) the promoting effect (11).

Since the most easily removed sulfur is at the S-edge in the MoS<sub>2</sub> structure, and since the Co is located at the S-edge, we first discuss the S-edge sulfur for the Co–Mo–S structure. The values of  $\Delta E_S$  for the Co–Mo–S structure are listed in Table 4. The S-edge in the Co–Mo–S structure is seen to have intrinsic vacancies as  $\Delta E_S = -70$  kJ/mol (going from  $a2$  to  $b2$  in Table 4). A half-stripped S-edge can also occur ( $b2 \rightarrow c2$  in Table 4).

A comparison of the values for the S-edge of the Co free system (Table 1) with the ones with Co in Table 4 reveals a

TABLE 4

Co-Mo-S Structures before and after Removal of Sulfur Atoms (The Corresponding Sulfur Binding Energy (per Sulfur Atom) Is Given. White, Light Grey, and Dark Grey Circles Denote S, Mo, and Co Atoms, Respectively. Dashed Circles Indicate S Atoms in the Bottom Layer. (US).)

S-edge, Co on S-edge					
Initial		Final		$\Delta E_S$	
Top View	Side View	Top View	Side View	(kJ/mol)	
<i>a2</i>		<i>b2</i>		-70	
<i>b2</i>		<i>c2</i>			
Mo-edge, Co on Mo-edge					
Initial		Final		$\Delta E_S$	
Top View	Side View	Top View	Side View	(kJ/mol)	
<i>e1</i>		<i>g1</i>		-62	
<i>g1</i>		<i>h1</i>			
				145	

clear reduction in  $\Delta E_S$  when S vacancies have a Co neighbor. (See Table 5.)

The configuration of the Co-Mo-S structure with one S atom removed from every super cell (*b2* in Table 4) is depicted in Fig. 3. The Mo-edge has dimerized S, while the S-edge has both S dimers and restructured S vacancies.

As in the case of the MoS<sub>2</sub> configurations, we also study the wider "3 Mo" structure for Co-Mo-S; see Fig. 2. The structure having one vacancy at the S-edge and no vacancies

at the Mo-edge is considered here. We initially split the S dimers at the Mo-edge, but after relaxation the structure eventually ends having the S dimers at this edge. Hence, in the "3 Mo" as well as in the "2 Mo" structures, the Mo-edge is covered by S dimers and the S-edge has both S dimers and vacancies.

In Table 3 it is seen that the bond lengths for Co-Mo-S have the same level of agreement with experiment as for the MoS<sub>2</sub> case. The too-short Mo-Mo and Mo-Co bond lengths for the "2 Mo" configuration is attributed to the narrow system used, but the experience from the MoS<sub>2</sub> case (see Sections 3.1 and 3.2) suggests that this effect is not important for the other calculated properties. In the calculated Co-Mo-S structures, the Co atoms appear to have more Mo neighbors than reported in the EXAFS experiments (38). However, one should be cautious to extract absolute numbers from these data since they are determined with great uncertainty.

Table 4 also shows that even though Co is less stable at the Mo-edge, the effect on the sulfur binding energy is the same. The energy required to make coordinatively unsaturated Mo atoms, which must be done by making an S

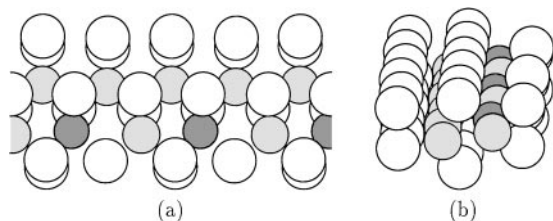


FIG. 3. The active Co-Mo-S configuration. Top view. The white circles denote S atoms, the light grey ones are Mo atoms, and the dark grey circles are Co atoms. (a) Top view, slightly tilted. (b) Side view, slightly tilted.

TABLE 5

Co-Mo-S Structures with Co Atom Placed at Either the S-Edge or the Mo-Edge (The Energy Difference,  $\Delta E$ , Is Presented. White, Light Grey, and Dark Grey Circles Denote S, Mo, and Co Atoms, Respectively. Dashed Circles Indicate S Atoms in the Bottom Layer. (US).)

At S-edge		
	Top View	$\Delta E$ (kJ/mol)
<i>f2</i>		0
At Mo-edge		
	Top View	$\Delta E$ (kJ/mol)
<i>g1</i>		55

vacancy starting from the half-covered Mo-edge (Table 4, e1) is considerably smaller than for the MoS<sub>2</sub> edge (Table 1).

## 6. COMPARISON OF THE EFFECT OF Co, Ni, AND Fe

We now turn to a comparison of the relative effects of Co, Ni, Fe, and Cu for the sulfided Mo catalyst in the HDS reaction. This is studied by comparing sulfur binding energies for removal of the first S atom at the S-edge, where the relevant transition metal is placed at the same site as the Co atom in configuration (1); see Table 6 in Section 4. After the metal substitution, all structures are allowed to relax. The results of the calculations are listed in Table 7, along with the unpromoted situation.

The promotional effect of both Co and Ni is evidenced from Table 7. Compared to MoS<sub>2</sub>,  $\Delta E_S$  is reduced substantially by the presence of these transition metals. The Co-Mo-S and Ni-Mo-S structures are seen to have intrinsic vacancies in the presence of H<sub>2</sub> and H<sub>2</sub>S (we return to the question of the effect of adsorbed hydrogen later). This suggests that these structures have high concentration of coordinatively unsaturated metal sites (CUS), except under extremely sulfiding conditions (as for configuration 1 in Table 6). The transition metal Fe is seen to be a very weak promoter for vacancy formation in the MoS<sub>2</sub> system, because Fe only lowers the sulfur binding energy by a small amount. This is in agreement with experimental results, since Fe addition only has a small effect on the catalytic

activity (see, e.g., (1)). The results of the calculations yield the same trends as the experimental observations, as depicted in Fig. 4.

In Table 7, Cu is seen to be a promoter for the MoS<sub>2</sub> system, whereas previous calculations (46, 47) suggest that Cu actually should act as a poison for the MoS<sub>2</sub> system. In the case of Cu, very little is known from experiments, and in (48) only separate Cu and Mo bulk sulfides were observed.

TABLE 6

Seven Different Possible Locations of Co in the Sulfided Co-Mo Structure (White, Light Grey, and Dark Grey Circles Denote S, Mo, and Co Atoms, Respectively. Dashed Circles Indicate S Atoms in the Bottom Layer. The Label of the Configuration Is Given by *n*. Quantities *x*, *y*, and  $\Delta E_n$  Are Described in the Text. In 1-3 Co Is Placed at the S-Edge. In 4-7, Co Is Situated at the Mo-Edge. (S).)

At S-edge				
<i>n</i>	Top View	<i>x</i>	<i>y</i>	$\Delta E_n$ (kJ/mol)
1		0	0	0
2		1	2	141
3		1	2	52
At Mo-edge				
<i>n</i>	Top View	<i>x</i>	<i>y</i>	$\Delta E_n$ (kJ/mol)
4		0	0	68
5		1	2	150
6		1	1	227
7		0	4	115



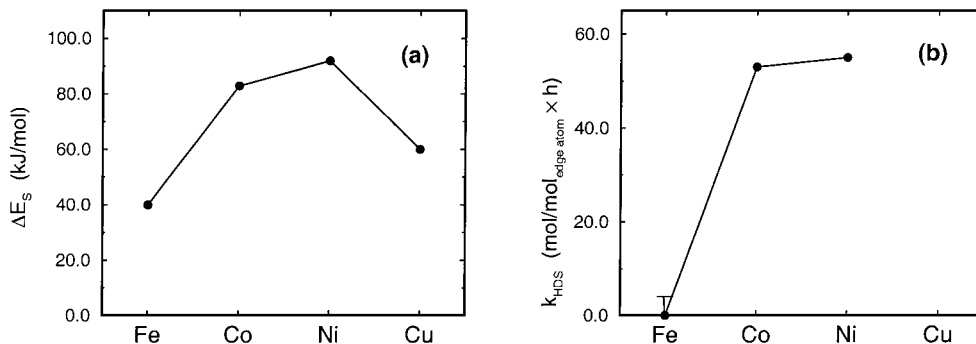


FIG. 4. The effect of different transition metals (Fe, Co, Ni, and Cu) on the activity of the sulfided Mo structure. The unpromoted MoS<sub>2</sub> structure is set as reference. (a) Calculated values of  $\Delta E_S$  (US). (b) Experimental values (1).

It may be that a Cu–Mo–S phase is not easily formed and that the effect measured is not a property of the Cu–Mo–S phase.

In order to understand why Co and Ni weakens the S bonding while Fe does so to a much lesser extent, we consider in Fig. 5 the projected density of *d* states (PDOS) on Mo, Fe, Co, and Ni atoms next to an S vacancy. It is the ability of these metal states to interact with the S valence states which determines the strength of the S bond (49). We need to understand why the interaction between the S 3*p* states and the Co and Ni *d* states is so much weaker than the interaction with the Fe *d* states.

The explanation goes in two steps. First, we note that when an adsorbate state, like one of the S 3*p* states (take a linear combination pointing towards the metal atom in question), interacts with a narrow band of metal *d* states, generally this results in the formation of bonding and antibonding states (49). This we illustrate by a simple molecular orbital (LCAO) model calculation where we concentrate on the interaction between S 3*p* states and the metal *d* states. Since the *d* states form a continuum of band states, as seen in Fig. 5, the LCAO model has to be modified as in the

so-called Newns–Anderson model (50, 51). Here we can model the interaction between any localized states (like the S 3*p* state) and a band of states with local projected DOS, for instance, on a Fe atom in Fe–Mo–S. The result of such a model calculation is shown in Fig. 6. All parameters used have been determined previously for S adsorption on metal surfaces (49). Note that for the case of an S 3*p* state interacting with the Fe *d*-states, the bonding combination is filled (i.e., completely below the Fermi level) while the antibonding state is only partly filled. This leads to a strong bond. This explains why S interacts strongly with a vacancy at the S-edge of Fe–Mo–S. This is completely different for Co–Mo–S and Ni–Mo–S. In Fig. 7, we compare the results from our model calculation of the S-projected DOS for the three cases. In contrast to the Fe case, the antibonding S-metal *d* states lie completely below the Fermi level for the Co and Ni promoted situations. When the bonding as well as the antibonding states are filled, the coupling is weak, and hence the S bond is much weaker for the Co and Ni promoted case than for the Fe promoted case.

TABLE 7

Calculated Sulfur Binding Energies for Unpromoted and Promoted Sulfided Mo Structures (Removal of the First S Atom from the S-Edge. (US).)

$\Delta E_S$ (kJ/mol)	
MoS <sub>2</sub>	13
Fe-Mo-S	- 27
Co-Mo-S	- 70
Ni-Mo-S	- 79
Cu-Mo-S	- 47

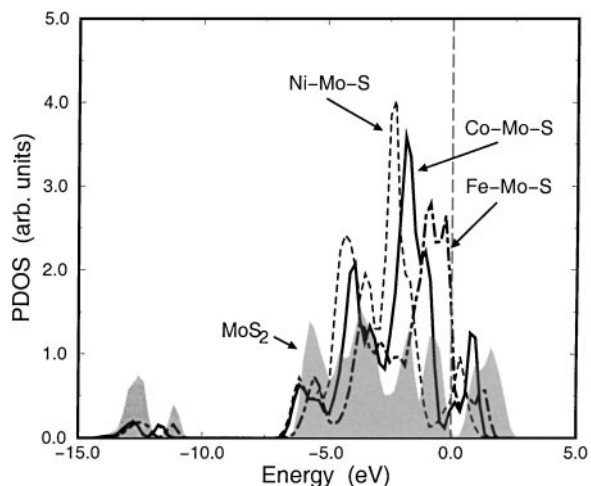
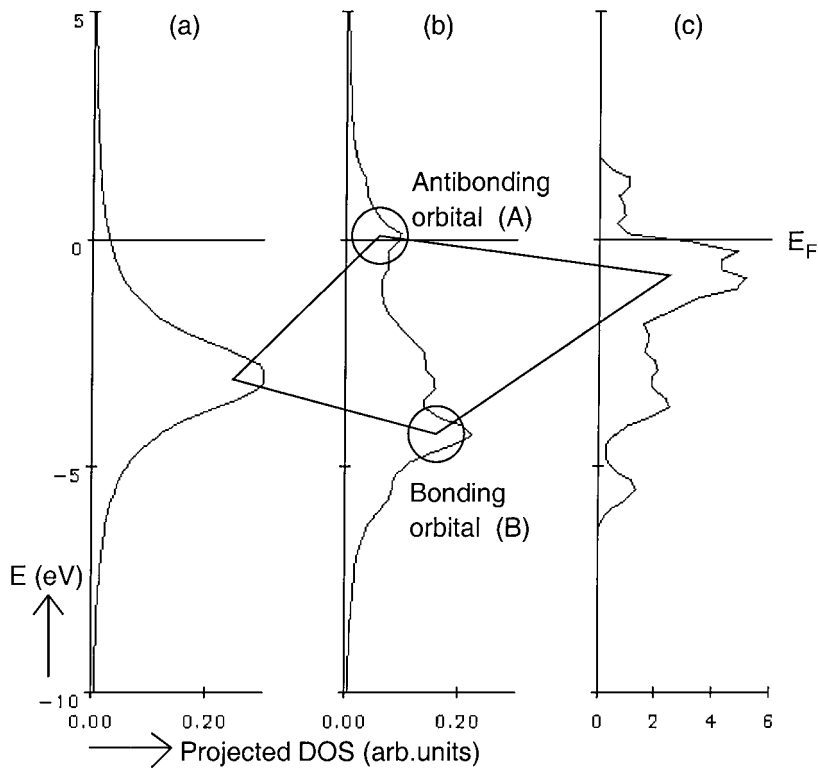
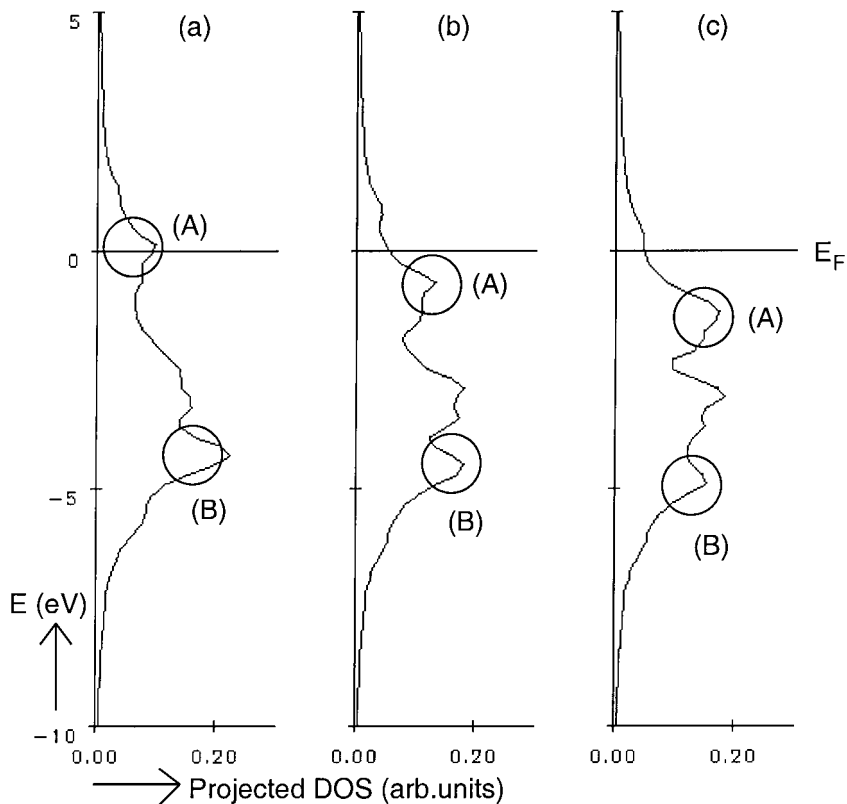


FIG. 5. The projected density of states for metal *d* states. The metal atoms, Fe, Co, and Ni, in the promoted structures are near the vacancy. The energy zero corresponds to the Fermi level. (S).



**FIG. 6.** Illustration of the Newns-Anderson model. (a) The renormalized  $S\ 3p$  states. (b) Result from the Newns-Anderson model. Antibonding (A) and bonding (B) orbitals are indicated. (c) The metal  $d$  band, in this case the Fe  $d$  band located in the Fe-Mo-S structure. (S).



**FIG. 7.** Results of interaction between  $S\ 3p$  states and metal  $d$  states. Antibonding (A) and bonding (B) orbitals are indicated. (a) Fe-Mo-S. (b) Co-Mo-S. (c) Ni-Mo-S. (S).

The pure Mo case cannot be compared directly to Fe, Co, and Ni because the coupling matrix elements between the  $d$  states of the  $4d$  metal Mo and the S valence states are considerably larger than for the  $3d$  metals (49).

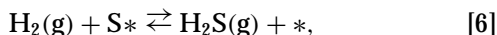
It is therefore a property of the  $d$ -states of the vacancy, cf. Fig. 5, that determines the strength of the interaction with an S atom. In particular it is seen that as the  $d$ -states move up in energy the antibonding states move up with them and thus become increasingly unoccupied (see Fig. 7). These results illustrate a general trend seen for metal surfaces that when the metal  $d$ -states move *up* in energy (towards the Fermi level), the interaction with adsorbates becomes stronger (52). It shows that concepts of chemisorption theory derived for metallic systems also apply to sulfides.

We thus suggest that an important effect of adding Co and Ni to the MoS<sub>2</sub> catalyst is to weaken the bonding of S to the S-edges. Coordinatively unsaturated metal atoms are hereby created, which can interact with thiophene or other sulfur-containing molecules.

These results clearly support the idea proposed in the Bond Energy Model (1, 11, 12), where one of the main roles of the promotor atoms is to create more vacancies. The detailed explanation of the effect is, however, somewhat different.

## 7. CO-MO-S STRUCTURE AND ATOMIC HYDROGEN

Apart from being able to bind the sulfur-bearing molecules the catalyst must be able to bind hydrogen in order to catalyze the HDS reaction. Hydrogen enters the HDS process through reactions like



where S\* denotes the “adsorbed” S atom and \* is a sulfur vacancy. Some H<sub>2</sub> molecules will dissociate on the surface of the Co-Mo-S structure (see, e.g., (12)), resulting in H atoms bound somewhere to the catalyst surface. These hydrogen atoms can for instance react with the S atom of an adsorbed organic molecule like thiophene, resulting in formation of H<sub>2</sub>S and a desulfurized molecule. Then H<sub>2</sub>S can be desorbed from the surface, regenerating the CUS.

In the present paper, we study the effect of atomic hydrogen on the Co-Mo-S surface, assuming dissociation of H<sub>2</sub> has already occurred. In all the studied Co-Mo-S structures, the Co atom is placed as in configuration 1, Table 6.

To study if atomic hydrogen is bound to the surface (with respect to H<sub>2</sub>), we write the following reaction:



In Eq. [7],  $A$  is a Co-Mo-S structure without hydrogen, while  $B$  is the structure with  $z$  adsorbed hydrogen atoms.  $A$  and  $B$  can be written as  $\text{Co}_a\text{Mo}_b\text{S}_c$  and  $\text{Co}_a\text{Mo}_b\text{S}_c\text{H}_z$ , respectively. Hence, the hydrogen binding energy per H

atom (relative to H<sub>2</sub>),  $\Delta E_{\text{H}}$ , is defined as

$$\Delta E_{\text{H}} = \frac{1}{z} \left( E(B) - E(A) - \frac{z}{2} E(\text{H}_2) \right), \quad [8]$$

where  $E(A)$  and  $E(B)$  are total energies of systems  $A$  and  $B$ . We thus have two cases, determined by the sign of  $\Delta E_{\text{H}}$ :

- For  $\Delta E_{\text{H}} > 0$ , atomic H is not bound to the surface, relative to H<sub>2</sub>.
- For  $\Delta E_{\text{H}} < 0$ , atomic H is bound. Negative values of  $\Delta E_{\text{H}}$  correspond to an energy gain.

We concentrate on the S-edge where Co is located, but note that we also attempted to adsorb atomic hydrogen on the basal plane of Co-Mo-S and found  $\Delta E_{\text{H}} = 94$  kJ/mol. In addition, our calculations show that molecular hydrogen, H<sub>2</sub>, desorbs from the basal plane, when the molecule is oriented perpendicular as well as parallel to the surface. Basal planes therefore cannot bind H<sub>2</sub> according to our calculations.

In Table 8, the results of the calculations are shown. Several structures  $a$ – $h$  have been considered, and we note that whenever hydrogen is adsorbed on a S dimer ( $a$  and  $c$ – $h$ ), we observe a splitting of the sulfur dimers.

If we now compare  $\Delta E_{\text{H}}$  for  $a$  and  $g$ , which has one and two H atoms on the S dimer, respectively, a strong interaction between H atoms perpendicular to the structure is seen. This implies that any kinetic model should include double sites. There is a simple reason for the apparently attractive interaction between the H atoms on adjacent S atoms. In all cases the S–S dimer bond must be broken to form the SH bonds. This costs some energy. When two SH groups are formed instead of one, the price of breaking the S–S bond per SH bond is only half and the SH bonds per H atoms are correspondingly stronger.

Interaction between H atoms along the Co-Mo-S chains seems at first different. The value of  $\Delta E_{\text{H}}$  for  $a$  and  $c$  is almost the same, indicating that the S dimer (with H) is not affected by the neighbor, i.e., whether there is an equivalent S dimer or a vacancy nearby. The value of  $\Delta E_{\text{H}}$  for  $g$  and  $h$  is also almost the same. We could furthermore imagine “adding” the structures  $a$  and  $b$  and obtaining configuration  $e$ . The sum of  $-22$  and  $+29$  is  $+7$ , which is close to the value of  $\Delta E_{\text{H}}$  for  $e$ , suggesting that interaction between H atoms along the structure is negligible. This is not always the case, though, as can be seen by comparing  $\Delta E_{\text{H}}$  for  $d$  with  $g$  and  $h$ . In  $d$  we see that the S dimer (with H atoms) is affected by the neighbor.

To find out where atomic hydrogen sits on the surface with a vacancy, we can compare  $a$  and  $b$ . It is seen that it costs energy to have H sit in the vacancy; see  $b$ . We have furthermore studied two situations where the H atom initially sits on either the Mo atom or the Co atom near the vacancy, which in both cases yields the final configuration and the value for  $\Delta E_{\text{H}}$  of structure  $b$ . Hence, a single

TABLE 8

The Effect of Atomic Hydrogen on the S-Edge of the Co-Mo-S Structure (The Number of H Atoms on the Structure (per Super Cell) is  $z$ . One and Zero Vacancies in the Co-Mo-S Structure Are Denoted  $\text{vac} = 1$  and  $\text{vac} = 0$ , Respectively. Configurations after Relaxation Are Depicted. The Hydrogen Binding Energy,  $\Delta E_H$ , Is Described in the Text. (S).)

$z$	$\text{vac}$	Label	Side View	$\Delta E_H$ (kJ/H)
1	1	<i>a</i>		- 22
		<i>b</i>		+ 29
2	0	<i>c</i>		- 20
		<i>d</i>		- 68
2	1	<i>e</i>		+ 2
		<i>f</i>		- 34
		<i>g</i>		- 38
4	0	<i>h</i>		- 36

hydrogen atom prefers to sit on an S atom and moves there if it starts on either Mo or Co.

Hydrogen therefore tends to form SH groups, and the case where both S atoms in a dimer has one H associated with it is by far the most stable.

Calculated bond lengths for "2 Mo" Co-Mo-S structures with adsorbed H are presented in Table 3. The configuration without vacancies (labelled No Vac.) is shown in Table 8, *h*, and the one with vacancies (With Vac.) is *g* in Table 8. It is seen that bond lengths agree reasonably with experiments (in the "2 Mo" limit) and differ only marginally from those for "2 Mo" Co-Mo-S without H.

## 8. FORMATION OF VACANCIES

We are now in a position to make a more complete description of vacancy formation at the S-edge of the structures. We concentrate on the most stable Co-Mo-S struc-

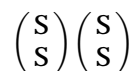
tures, *d*, *g*, and *h* in Table 8. The effective H-H interactions along and perpendicular to the chains means that we have to consider at least four S atoms or S adsorption sites in our analysis. Figure 8 is an energy diagram of different sulfidation and hydrogenation states of Co-Mo-S and MoS<sub>2</sub> structures, for which the new nomenclature is defined.

$\begin{pmatrix} \text{S} \\ \text{S} \end{pmatrix}$ : Two S atoms (e.g., in an S dimer) at the edge.

$\begin{pmatrix} \text{SH} \\ \text{SH} \end{pmatrix}$ : Two SH groups at the edge.

(S): A single S atom and a vacancy at the edge.

The sulfided structure ①, written as



is chosen as reference and the energies of the different possible intermediates are collected in Fig. 8. Note that  $\Delta E_H$  is defined per H atom (see Eq. [8]). Hence, process ① → ②

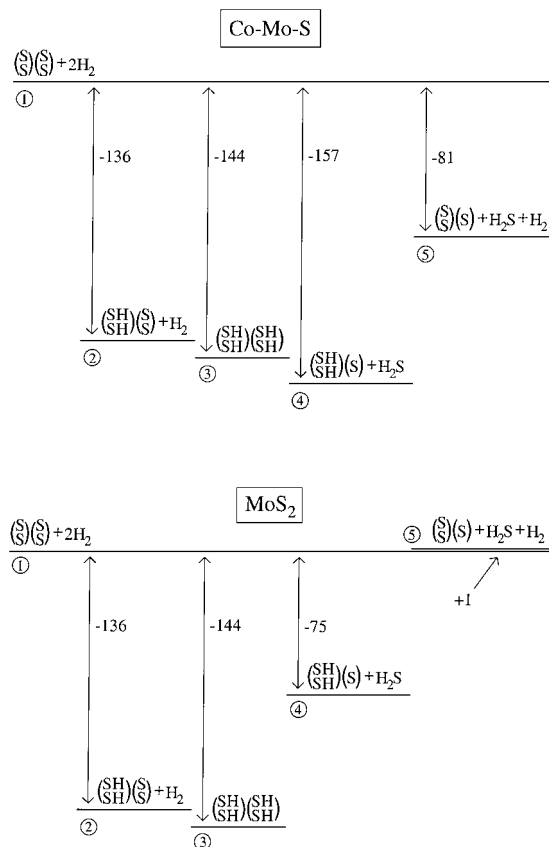


FIG. 8. Energy diagram of different sulfidation and hydrogenation states of Co-Mo-S and MoS<sub>2</sub> structures. The reference value is chosen to belong to the completely sulfided structure without vacancies plus two hydrogen molecules in the gas phase. Values are given in kJ/mol. (S).

corresponds to  $2(\Delta E_{\text{H}})$  (see Table 8, *d*), step ① → ③ is  $4(\Delta E_{\text{H}})$  (see Table 8, *h*), and process ① → ④ is  $2(\Delta E_{\text{H}}) + \Delta E_{\text{S}}$  (see Table 8, *g* and Table 7). These values are only calculated for the Co–Mo–S structure, while the results for MoS<sub>2</sub> are based on the assumption that the strength of the SH bond is not dependent on the kind of structure considered. In step ① → ⑤, the sulfur binding energy,  $\Delta E_{\text{S}}$ , is used (see Table 7).

For the Co–Mo–S structure, it is seen from Fig. 8 that the most stable configuration is one with vacancies and SH groups on the remaining S “dimers” ④. The fully hydrogenated edge with no vacancies ③ is almost as stable, while the completely hydrogen-free edge ① is considerably less stable. The structure with H atoms on every second dimer ② is almost as stable as the fully hydrogenated structure (the same energy to within our accuracy).

For the MoS<sub>2</sub> case, the fully hydrogenated edge ③ seems most stable, while the partly hydrogenated edge ④ with vacancies is about 70 kJ/mol higher in energy.

The calculations suggest that the edges of the catalyst are at least partly hydrogenated during synthesis conditions. This agrees with IR measurements of the catalysts (53, 54). The calculations also suggest that adding Co increases the number of vacancies, and since H does not bind to the remaining S atoms at the vacancy, the amount of adsorbed hydrogen should decrease with Co promotion. Such an effect has been observed experimentally (53, 54).

## 9. SUMMARY

In the present paper, we have applied DFT calculations to study unpromoted and promoted MoS<sub>2</sub>-based catalysts used in the hydrodesulfurization reaction. The following has been found:

- For unpromoted MoS<sub>2</sub> catalysts, a nonstoichiometric configuration with S restructuring at both edges has been found to be most stable. The (1010) Mo-edge is filled by one or two S atoms per Mo edge atom. However, in both cases the S coordination number is six for the Mo edge atoms. Vacancies are most easily created at the (1010) S-edge. Bond lengths are found to agree very well with experiments.

- The location of Co at the MoS<sub>2</sub> edges in the Co–Mo–S structures has been investigated. Contrary to previous models, the results reveal that Co prefers to substitute some Mo atoms at the S-edge. Studies of S bonding in the Co–Mo–S structure result in a model with vacancies near Co atoms at the S-edge. The sulfur binding energy is reduced by the presence of Co atoms. The Mo-edge has dimerized S, while the S-edge has S dimers as well as S vacancies. Calculated bond lengths are again found to agree with experimental values. The stability of this vacancy-containing Co–Mo–S model is compared with bulk cobalt sulfide, and Co–Mo–S appears to be the more stable structure under typical catalytic conditions.

- The role of different promoters for the MoS<sub>2</sub> structure is studied, and it is revealed that Co and Ni atoms increase the activity of the catalyst, while Fe is an extremely weak promoter, in agreement with experiments. The promotional effect is also modelled by use of the Newns–Anderson model, and from this it is seen that for Co–Mo–S and Ni–Mo–S the antibonding state lies below the Fermi level. Hence, these structures bind S atoms weakly, resulting in formation of vacancies, where S-bearing molecules then can be adsorbed. In contrast, the antibonding state for the Fe–Mo–S configuration is partly above the Fermi level, resulting in stronger S bonding. Fewer vacancies will thus be present in the Fe–Mo–S structures.

- The adsorption of atomic hydrogen on Co–Mo–S structures is studied. It is found that when hydrogen is adsorbed on S dimers, these dimers split. A strong interaction between H atoms perpendicular to the slabs is found, and in some cases interaction is found along the chains too. A single H atom prefers to sit on an S atom instead of being bonded to Mo or Co atoms near a vacancy.

- The study of formation of vacancies at the S-edges of the structures must include at least four S adsorption sites. In the Co–Mo–S case, the most stable structure has vacancies and SH groups on the S dimers. A fully hydrogenated structure is almost as stable. In the MoS<sub>2</sub> situation, the fully hydrogenated structure is found to be most stable, in agreement with experiments.

## 10. ACKNOWLEDGMENTS

The present work was in part financed by The Danish Research Councils through The Center for Surface Reactivity and grant 9501775. The Center for Atomic-Scale Materials Physics is sponsored by the Danish National Research Foundation.

## REFERENCES

1. Topsøe, H., Clausen, B. S., and Massoth, F. E., in “Hydrotreating Catalysis, Science and Technology” (J. R. Anderson and M. Boudart, Eds.), Vol. 11. Springer-Verlag, Berlin/New York, 1996.
2. Sonnemans, J. W. M., in “Catalysts in Petroleum Refining and Petrochemical Industries 1995” (M. Absi-Halabi *et al.*, Eds.), p. 99. Elsevier Science B. V., Amsterdam/New York, 1996.
3. Gosselink, J. W., in “Transition Metal Sulphides” (T. Weber, R. Prins, and R. A. van Santen, Eds.), p. 311. Kluwer Academic, Dordrecht/Norwell, MA, 1998.
4. Mochida, I., Sakanishi, K., Ma, X., Nagao, S., and Isoda, T., *Catal. Today* **29**, 185 (1996).
5. Whitehurst, D. D., Isoda, T., and Mochida, I., *Adv. Catal.* **42**, 343 (1998).
6. Landau, M. V., *Catal. Today* **36**, 393 (1997).
7. Gates, B. C., and Topsøe, H., *Polyhedron* **16**, 3213 (1997).
8. Topsøe, H., Knudsen, K. G., Byskov, L. S., Nørskov, J. K., and Clausen, B. S., *Catal. Today*, in press.
9. Prins, R., de Beer, V. H. J., and Somorjai, G. A., *Catal. Rev. Sci. Eng.* **31**, 1 (1989).
10. Hensen, E., and van Santen, R. A., *Cattech.* **3**, 86 (1998).
11. Nørskov, J. K., Clausen, B. S., and Topsøe, H., *Catal. Lett.* **13**, 1 (1992).
12. Topsøe, H., Clausen, B. S., Topsøe, N.-Y., Nørskov, J. K., Ovesen, C. V., and Jacobsen, C. J. H., *Bull. Soc. Chim. Belg.* **104**, 283 (1995).

13. Byskov, L. S., Nørskov, J. K., Clausen, B. S., and Topsøe, H., in "Transition Metal Sulphides" (T. Weber, R. Prins, and R. A. van Santen, Eds.), p. 155. Kluwer Academic, Dordrecht/Norwell, MA, 1998.
14. Neurock, M., and van Santen, R. A., *J. Am. Chem. Soc.* **116**, 4427 (1994).
15. Byskov, L. S., Hammer, B., Nørskov, J. K., Clausen, B. S., and Topsøe, H., *Catal. Lett.* **47**, 177 (1997).
16. Byskov, L. S., Nørskov, J. K., Clausen, B. S., and Topsøe, H., *ACS Petrol. Div. Prepr.* **43**(1), 12 (1998).
17. Raybaud, P., Kresse, G., Hafner, J., and Toulhoat, H., *J. Phys. Condens. Matter* **9**, 11085 (1997).
18. Raybaud, P., Hafner, J., Kresse, G., and Toulhoat, H., *J. Phys. Condensed Matter* **9**, 11107 (1997).
19. Faye, P., Payen, E., and Bougeard, D., *J. Catal.* **179**, 560 (1998).
20. Harris, S., and Chianelli, R., in "Theoretical Aspects of Heterogeneous Catalysis" (J. B. Moffat, Ed.), Van Nostrand-Reinhold, New York, 1990.
21. Zonnevylle, M. C., Hoffmann, R., and Harris, S., *Surf. Sci.* **199**, 320 (1988).
22. Burdett, J. K., and Chung, J. T., *Surf. Sci. Lett.* **236**, L353 (1990).
23. Mitchell, P. C. H., and Plant, C., *Bull. Soc. Chim. Belg.* **104**, 293 (1995).
24. Hammer, B., Hansen, L. B., and Nørskov, J. K., *Phys. Rev. B*, to appear.
25. Perdew, J. P., Chevary, J. A., Vosko, S. H., Jackson, K. A., Pedersen, M. R., Singh, D. J., and Fiolhais, C., *Phys. Rev. B* **46**, 6671 (1992).
26. Troullier, N., and Martins, J. L., *Phys. Rev. B* **43**, 1993 (1991).
27. Vanderblit, D., *Phys. Rev. B* **41**, 7892 (1990).
28. Ibach, H., and Lüth, H., "Solid-State Physics." Springer-Verlag, Berlin/New York, 1993.
29. Ashcroft, N. W., and Mermin, N. D., "Solid State Physics." Saunders, Philadelphia, 1976.
30. Topsøe, H., and Clausen, B. S., *Catal. Rev. Sci. Eng.* **26**, 395 (1984).
31. Topsøe, H., Topsøe, N.-Y., Sørensen, O., Candia, R., Clausen, B. S., Kallesøe, S., and Pedersen, E., *Am. Chem. Soc. Div. Petrol. Prepr.* **28**, 1252 (1994).
32. Polz, J., Zeilinger, H., Müller, B., and Knözinger, H., *J. Catal.* **120**, 22 (1989).
33. Muijsers, J. C., Weber, T., van Hardeveld, R. M., Zandbergen, H. W., and Niemantsverdriet, J. W., *J. Catal.* **157**, 698 (1995).
34. Duchet, J. C., van Oers, E. M., de Beer, V. H. J., and Prins, R., *J. Catal.* **80**, 386 (1983).
35. Salmeron, M., Somorjai, G. A., Wold, A., Chianelli, R., and Liang, K. S., *Chem. Phys. Lett.* **90**, 105 (1982).
36. Clausen, B. S., Topsøe, H., Candia, R., Villadsen, J., Lengeler, B., Als-Nielsen, J., and Christensen, F., *J. Phys. Chem.* **85**, 3868 (1981).
37. Topsøe, H., Clausen, B. S., Topsøe, N.-Y., and Zeuthen, P., *Stud. Surf. Sci. Catal.* **53**, 77 (1989).
38. Bouwens, S. M. A. M., van Veen, J. A. R., Koningsberger, D. C., de Beer, V. H. J., and Prins, R., *J. Phys. Chem.* **95**, 123 (1991).
39. Raybaud, P., Hafner, J., Kresse, G., and Toulhoat, H., *Surf. Sci.* **407**, 237 (1998).
40. Niemann, W., Clausen, B. S., and Topsøe, H., *Catal. Lett.* **4**, 355 (1990).
41. Bouwens, S. M. A. M., Koningsberger, X. D. C., de Beer, V. H. J., Louwers, S. P. A., and Prins, R., *Catal. Lett.* **5**, 273 (1990).
42. Louwers, S. P. A., and Prins, R., *J. Catal.* **133**, 94 (1992).
43. Startsev, A. N., *Catal. Rev. Sci. Eng.* **37**, 353 (1995).
44. Delmon, B., *Stud. Surf. Sci. Catal.* **53**, 1 (1990).
45. Schönberg, N., *Acta Metall.* **2**, 427 (1954).
46. Harris, S., and Chianelli, R. R., *J. Catal.* **98**, 17 (1986).
47. Chianelli, R. R., Daage, M., and Ledoux, M. J., *Adv. Catal.* **40**, 177 (1994).
48. Kulkarni, G. U., and Rao, C. N. R., *Catal. Lett.* **9**, 427 (1991).
49. Hammer, B., and Nørskov, J. K., in "Chemisorption and Reactivity on Supported Clusters and Thin Films" (R. M. Lambert and G. Pacchioni, Eds.), p. 285. Kluwer Academic, Dordrecht/Norwell, MA, 1997.
50. Newns, D. M., *Phys. Rev.* **178**, 1123 (1969).
51. Anderson, P. W., *Phys. Rev.* **124**, 41 (1961).
52. Mavrikakis, M., Hammer, B., and Nørskov, J. K., *Phys. Rev. Lett.* **81**, 2819 (1998).
53. Topsøe, N.-Y., Topsøe, H., and Massoth, F. E., *J. Catal.* **119**, 252 (1989).
54. Topsøe, N.-Y., and Topsøe, H., *J. Catal.* **139**, 641 (1993).